NEOPLASIA
www.neoplasia.com
Volume 11 Number 9 September 2009 pp. 846–855 846

Loss of Endogenous Interleukin-12 Activates Survival Signals in Ultraviolet-Exposed Mouse Skin and Skin Tumors[1]

Syed M. Meeran*, Nandan Katiyar*, Tripti Singh* and Santosh K. Katiyar*,†

*Department of Dermatology, University of Alabama at Birmingham, Birmingham, AL 35294, USA; †Birmingham VA Medical Center, Birmingham, AL 35294, USA

Abstract

Interleukin-12 (IL-12)–deficiency promotes photocarcinogenesis in mice; however, the molecular mechanisms underlying this effect have not been fully elucidated. Here, we report that long-term exposure to ultraviolet (UV) radiation resulted in enhancement of the levels of cell survival kinases, such as phosphatidylinositol 3-kinase (PI3K), Akt (Ser^{473}), p-ERK1/2, and p-p38 in the skin of IL-12p40 knockout (IL-12 KO) mice compared with the skin of wild-type mice. UV-induced activation of nuclear factor-κB (NF-κB)/p65 in the skin of IL-12 KO mice was also more prominent. The levels of NF-κB–targeted proteins, such as proliferating cell nuclear antigen (PCNA), cyclooxygenase-2, cyclin D1, and inducible nitric oxide synthase, were higher in the UV-exposed skin of IL-12 KO mice than the UV-exposed skin of wild types. In short-term UV irradiation experiments, subcutaneous treatment of IL-12 KO mice with recombinant IL-12 (rIL-12) or topical treatment with oridonin, an inhibitor of NF-κB, resulted in the inhibition of UV-induced increases in the levels of PCNA, cyclin D1, and NF-κB compared with non–rIL-12– or non–oridonin-treated IL-12 KO mice. UV-induced skin tumors of IL-12 KO mice had higher levels of PI3K, p-Akt (Ser^{473}), p-ERK1/2, p-p38, NF-κB, and PCNA and fewer apoptotic cells than skin tumors of wild types. Together, these data suggest that the loss of endogenous IL-12 activates survival signals in UV-exposed skin and that may lead to the enhanced photocarcinogenesis in mice.

Neoplasia (2009) 11, 846–855

Introduction

Interleukin-12 (IL-12) is a pleiotropic cytokine that is secreted by activated professional antigen presenting cells [1]. Previously, we and others have shown that IL-12p40–deficiency enhances photocarcinogenesis in mice in tumor incidence, tumor multiplicity, and the extent of tumor angiogenesis [2–4]. IL-12 possesses antitumor activity, enhances antitumor immunity, and can repair ultraviolet (UV)-induced DNA damage in the form of cyclobutane pyrimidine dimers [1,2,5,6].

It has been reported that several signal transduction pathways, which mediate cell proliferation, transformation, and cell death, are involved in UV radiation–induced skin carcinogenesis [7]. UVB radiation–induced signaling events are primarily mediated through mitogen-activated protein kinases (MAPKs) and activation of transcription factors, such as nuclear factor-κB (NF-κB) [8,9]. The activation of MAPKs by UVB plays a significant role in tumor promotion and malignant transformation [9]. Furthermore, Akt, a prosurvival factor that is the downstream serine/threonine kinase of phosphatidylinositol-3-kinase (PI3K) family members, is critical for UVB-induced tumor promotion and tumor cell survival [10]. Akt can activate various antiapoptotic proteins including NF-κB and can inactivate several proapoptotic proteins, including Bad and caspase 9 [11]. It has been documented that NF-κB is a downstream target of the MAPK signal transduction pathway and that the activation of NF-κB plays a crucial role in inflammation, cellular proliferation, and induction of cancers. Many studies have shown the constitutive up-regulation of NF-κB in a variety of tumor cells [12–14]. Consequently, the NF-κB activating pathway is a major target for the development of alternative anticancer agents/drugs.

Abbreviations: IL, interleukin; IL-12 KO, interleukin-12 knock out; COX-2, cyclooxygenase-2; NF-κB, nuclear factor-κB; PCNA, proliferating cell nuclear antigen; PI3K, phosphatidylinositol 3-kinase; UV, ultraviolet

Address all correspondence to: Santosh K. Katiyar, PhD, Department of Dermatology, University of Alabama at Birmingham, 1670 University Blvd, Volker Hall 557, PO Box 202, Birmingham, AL 35294. E-mail: skatiyar@uab.edu

[1]This work was supported by grants from the National Center for Complementary and Alternative Medicine/NIH (1 RO1 AT002536; S.K.K.) and the Veterans Administration Merit Review Award (S.K.K.). No conflict of interest.
Received 25 March 2009; Revised 22 May 2009; Accepted 26 May 2009

DOI 10.1593/neo.09528

In this study, we therefore focused our attention on examining the possible role of IL-12 deficiency on cell survival signals in photocarcinogenesis by the analysis of UVB-exposed skin and UVB-induced skin tumors in IL-12–deficient or IL-12 knockout (IL-12 KO) mice, and resultant data were compared with their wild-type IL-12–proficient counterparts. Using immunohistochemical analysis, Western blot analysis, and real-time polymerase chain reaction (PCR), we demonstrate that long-term UVB exposure results in enhanced up-regulation of cell survival kinases, including PI3K, p-Akt, and MAPK, in the skin of the IL-12 KO mice compared with the skin of the wild-type mice. Similar enhancement of cell survival kinase activity and NF-κB signaling in the UV-induced skin tumors in the IL-12 KO mice suggests that a loss of endogenous IL-12 activates cell survival signals and that may lead to enhanced photocarcinogenesis in mice.

Materials and Methods

Chemicals and Antibodies

Antibodies specific for caspase 3, caspase 9, Akt, p-Akt, p-Bad, Bad, MAPKs, NF-κB, IKKα, and IκBα were purchased from Cell Signaling (Danvers, MA). Oridonin, an inhibitor of NF-κB, was obtained from Calbiochem (San Diego, CA). Immunostaining-specific proliferating cell nuclear antigen (PCNA) antibody and all other secondary antibodies were obtained from Santa Cruz Biotechnology, Inc (Santa Cruz, CA). Anti-PI3K, inducible nitric oxide synthase (iNOS), and cyclooxygenase-2 (COX-2) antibodies were obtained from Cayman Chemicals (Ann Arbor, MI). The protein assay kit was obtained from Bio-Rad (Hercules, CA), and the enhanced chemiluminescence Western blot analysis detection reagents were purchased from Amersham Pharmacia Biotech (Piscataway, NJ). Terminal deoxynucleotide transferase (TdT)–mediated dUTP-biotin nick end-labeling (TUNEL) assay system was obtained from Promega (Madison, WI). The endotoxin-free mouse recombinant IL-12 (rIL-12) was purchased from eBioscience (San Diego, CA). All other chemicals were purchased from Sigma Chemical, Co (St Louis, MO).

Animals

Pathogen-free female C3H/HeN mice (6-7 weeks old) were purchased from The Jackson Laboratory (Bar Harbor, ME). The IL-12p40 KO mice on a C3H/HeN background were generated in our Animal Resource Facility as described previously [2]. The mutation in the p40 chain of IL-12 in IL-12 KO mice completely eliminates the synthesis of biologically active IL-12. All mice were maintained under standard conditions: 12-hour dark/12-hour light cycle, 24 ± 2°C temperature, and 50 ± 10% relative humidity. The mice were fed the Purina Taklad diet (Harlan Teklad, Madison, WI) and water *ad libitum*. The experimental animal protocol was approved by institutional animal care and use committee of the University of Alabama at Birmingham.

UV Irradiation of Mice

Mice were exposed to UV radiation as described previously [2,4]. Briefly, the clipper-shaved dorsal skin was exposed to UV radiation from a band of four FS24 T1 UVB lamps (Daavlin, UVA/UVB Research Irradiation Unit, Bryan, OH) equipped with an electronic controller to regulate UV dosage. The UV lamps primarily emit UVB (290-320 nm, >80% of total energy) and UVA (320-375 nm, <20% of total energy) radiation with peak emission at 314 nm as monitored [2]. The UVB emission was also monitored regularly using a UV radiometer (Daavlin, Bryan, OH).

Photocarcinogenesis Protocol

A photocarcinogenesis protocol was used as described earlier [2,15]. Briefly, mice were UVB irradiated everyday (180 mJ/cm^2) for a total of 10 days to stimulate tumor initiation. One week after the last UVB exposure of the tumor initiation stage, the mice were irradiated with the same dose of UVB thrice weekly until the end of the protocol to stimulate tumor promotion. The number of mice in each UVB-exposed group (IL-12 KO or WT) was 20. The UVB-irradiated dorsal skin of the mice was examined on a weekly basis for papillomas or tumor appearance. Growths greater than 1 mm in diameter that persisted for at least 2 weeks were defined as tumors and recorded. Tumor data for each mouse were recorded until the yield and tumor size stabilized. Control groups of mice (IL-12 KO and WT), which were age- and sex-matched with the experimental groups, were not exposed to UVB (sham irradiated, n = 20).

Evaluation of Tumor Size

At the termination of the photocarcinogenesis experiment, the tumor data on each mouse were recorded. The dimensions of all the tumors on each mouse were measured, and tumor volumes were calculated using the hemiellipsoid model formula: tumor volume = 1/2 (4π/3) (l/2) (w/2) h, where l = length, w = width, and h = height.

Short-term UV Exposure Protocol

For short-term UV exposure, the mice were exposed to UVB (90 mJ/cm^2) on alternate days for a total of three exposures and killed 24 hours after the last UVB exposure. IL-12 KO mice were assigned randomly to one of four groups (n = 5 per group). Group 1, mice were exposed to UVB. Group 2, mice were injected subcutaneously with endotoxin-free murine rIL-12 (1000 ng/100 μl PBS) on the shaved back 3 hours before each UVB exposure. Group 3, mice were treated topically with oridonin (20 μmol/100 μl acetone) as described [16], on the shaved back approximately 30 minutes before each UVB exposure. Group 4, non–UVB-exposed control mice, which were injected with 100 μl of sterile saline subcutaneously before each sham irradiation.

Preparation of Tumor and Skin Lysates and Western Blot Analysis

Skin and tumor lysates for Western blot analysis were prepared as described previously [4,8]. The tissue samples were pooled from at least three mice in each group, and three sets of pooled samples from each treatment group were used to prepare lysates, thus n = 9 to 10. Briefly, proteins (30-50 μg) were resolved on 10% Tris-glycine gel and transferred onto nitrocellulose membranes. Membranes were incubated in blocking buffer for 1 hour at room temperature and then incubated with the primary antibodies in blocking buffer overnight at 4°C. The membrane was then washed with PBS buffer and then incubated with secondary antibody conjugated with horseradish peroxidase (HRP). Protein bands were visualized using enhanced chemiluminescence detection reagents (Amersham Life Science, Inc, Piscataway, NJ). To verify equal protein loading and transfer of proteins from gel to membrane, the blots were stripped and reprobed for β-actin.

Immunohistochemical Detection of Caspase 3 and PCNA Proteins

Tissue samples were placed in 10% neutral-buffered formalin, processed, and embedded in paraffin blocks. Tissue sections (5 μm thick)

were deparaffinized and rehydrated in a graded series of alcohols. After rehydration, an antigen-retrieval process was performed by placing the slides in 10 mM sodium citrate, pH 6.0, at 95°C for 20 minutes followed by a 20-minute cooling step as described [17]. The sections were washed in PBS, and nonspecific binding sites were blocked with 1% BSA with 2% goat serum in PBS. The sections were incubated with an anti–caspase 3 or anti-PCNA antibody for 1 hour at room temperature. The sections were washed and incubated with the appropriate secondary antibody conjugated with HRP for 30 minutes. After washing in PBS, sections were incubated with diaminobenzidine and counterstained with hematoxylin and eosin. The numbers of PCNA-positive and caspase 3–positive cells were counted in at least at five different fields. Representative photomicrographs were obtained using a Qcolor5 digital camera attached to an Olympus BX41 microscope (Olympus, Tokyo, Japan).

NF-κB/p65 Activity Assay

For quantitative analysis of NF-κB/p65 activity, NF-κB Trans^{AM} Activity Assay Kit (Active Motif, Carlsbad, CA) was used following the manufacturer's protocol. For this assay, the nuclear extracts of epidermal skin samples from various treatment groups were prepared using the Nuclear Extraction Kit (Active Motif) according to the manufacturer's direction. Absorbance was recorded at 450 nm with reference taken at 650 nm. The results are expressed as the percentage OD of control (non–UVB-exposed) group.

Detection of Apoptotic Cells Using the TUNEL Assay

Tumor sections (5 μm thick) were stained for apoptosis by *in situ* labeling of DNA breaks using the TUNEL method according to the manufacturer's protocol (Promega). Briefly, after deparaffinization and hydration, the sections were incubated with proteinase K (20 μg/ml) for 15 minutes at room temperature and washed with PBS followed by fixation using 4% paraformaldehyde. The sections were equilibrated with rTdT reaction mixture (25 mM Trizma base pH 6.6, 200 mM potassium cacodylate pH 6.6, 0.2 mM DTT, 0.25 mg/ml BSA, and 2.5 mM cobalt chloride) for 10 minutes. The sections were then covered with the biotinylated nucleotide mixture (1 μl/100 μl rTdT mix) and the rTdT enzyme mixture (1 μl/100 μl rTdT mix) in rTdT buffer and incubated in a humidified chamber at 37°C for 60 minutes. The reaction was terminated by transferring the slides into 2× SSC buffer for 15 minutes at room temperature. Endogenous peroxidase was inactivated by incubating with 0.3% H_2O_2 for 5 minutes. The sections were rinsed with PBS and incubated with streptavidin-HRP (1:500 vol/vol) for 30 minutes. After washing in PBS, the sections were incubated with diaminobenzidine substrate solution with peroxidase and counterstained with Harris hematoxylin (Sigma Chemical, Co). The numbers of TUNEL-positive cells were counted using an Olympus BX41 microscope, $n = 6$. Representative photomicrographs were obtained using a Qcolor5 digital camera system fitted to an Olympus BX41 microscope.

RNA Extraction and Quantitative Real-time PCR

Total RNA was extracted from samples of the mouse epidermis using TRIzol reagents (Invitrogen, Carlsbad, CA) following the protocol recommended by the manufacturer. The concentration of total RNA was determined by measuring the absorbance at 260 nm using a Beckman/Coulter DU 530 spectrophotometer (Fullerton, CA). The expression of PCNA messenger RNA (mRNA) and cyclin D1 mRNA was estimated using real-time PCR. For mRNA quantification, complementary DNA (cDNA) was synthesized using 1 μg of RNA through a reverse transcription reaction (iScript cDNA Synthesis Kit; Bio-Rad). Using the SYBR Green/Fluorescein PCR Master Mix (SuperArray Bioscience, Corp, Frederick, MD), cDNA was amplified using real-time PCR with a Bio-Rad MyiQ thermocycler and SYBR Green detection system. Samples were run in triplicate to ensure amplification integrity. Manufacturer-supplied primer pairs (SuperArray Bioscience, Corp) were used to estimate the mRNA levels of PCNA, cyclin D1, COX-2, iNOS, and β-actin. The standard PCR conditions were as follows: 95°C for 15 minutes, then 40 cycles at 95°C for 30 seconds; 55°C for 30 seconds and 72°C for 30 seconds, as recommended by the manufacturer of the primers. The expression levels were normalized to that of the β-actin mRNA in each sample. The threshold for positivity of real-time PCR was determined based on negative controls. For mRNA analysis, calculations for determining the relative level of gene expression were made using the cycle threshold (C_t) method. The mean C_t values from duplicate measurements were used to calculate the expression of the target gene with normalization to the housekeeping gene used as internal control (*β-actin*), and using the $2^{-\Delta Ct}$ formula.

Statistical Analysis

The results are expressed as the mean ± SD. The statistical significance of difference between the values of treatment groups was determined using analysis of variance followed by *post hoc* Tukey test. $P < .05$ was considered statistically significant.

Results

IL-12 Deficiency Enhances Photocarcinogenesis in Mice

Because IL-12 has been shown to possess antitumor activity [18], we determined the effect of IL-12 deficiency on susceptibility to UVB-induced skin carcinogenesis. Following the photocarcinogenesis protocol, we found that UVB-induced tumor development occurred 14 days earlier in IL-12 KO mice than their wild-type counterparts (Figure 1*A*). In tumor multiplicity, the total number of tumors in the group of IL-12 KO mice ($n = 20$) remained higher than the total number of tumors in the group of wild-type mice throughout the experimental protocol (Figure 1*A*). At the termination of the experiment, the total number of tumors was significantly higher in the group of IL-12 KO mice ($P < .001$) than the group of wild-type mice. The tumor volume or size was significantly higher in the group of IL-12 KO mice compared with their wild types ($P < .001$; Figure 1*B*) at the termination of the photocarcinogenesis experiment [2]. These data clearly indicate that IL-12–deficient mice are susceptible to UVB-induced skin carcinogenesis.

IL-12 Deficiency Activates PI3K/Akt Signaling Pathway in UV-Irradiated Skin

The risk of photocarcinogenesis can be increased through various signaling pathways including the activation of cell survival kinases [7,9,10]. Studies have shown that the activation of PI3K plays an important role in tumor promotion and carcinogenesis [19–21]. To investigate which signaling pathways are activated in UV-exposed skin in the absence of IL-12, we examined the kinases PI3K/Akt, p38 MAPK, and ERK1/2 in skin samples from UVB-exposed IL-12 KO mice and UVB-exposed wild-type mice using Western blot analysis. We found that the basal levels of PI3K proteins were higher in the non–UV-exposed skin of IL-12 KO mice than in the non–UV-exposed skin of WT mice. As expected, the levels of both the catalytic (p110)

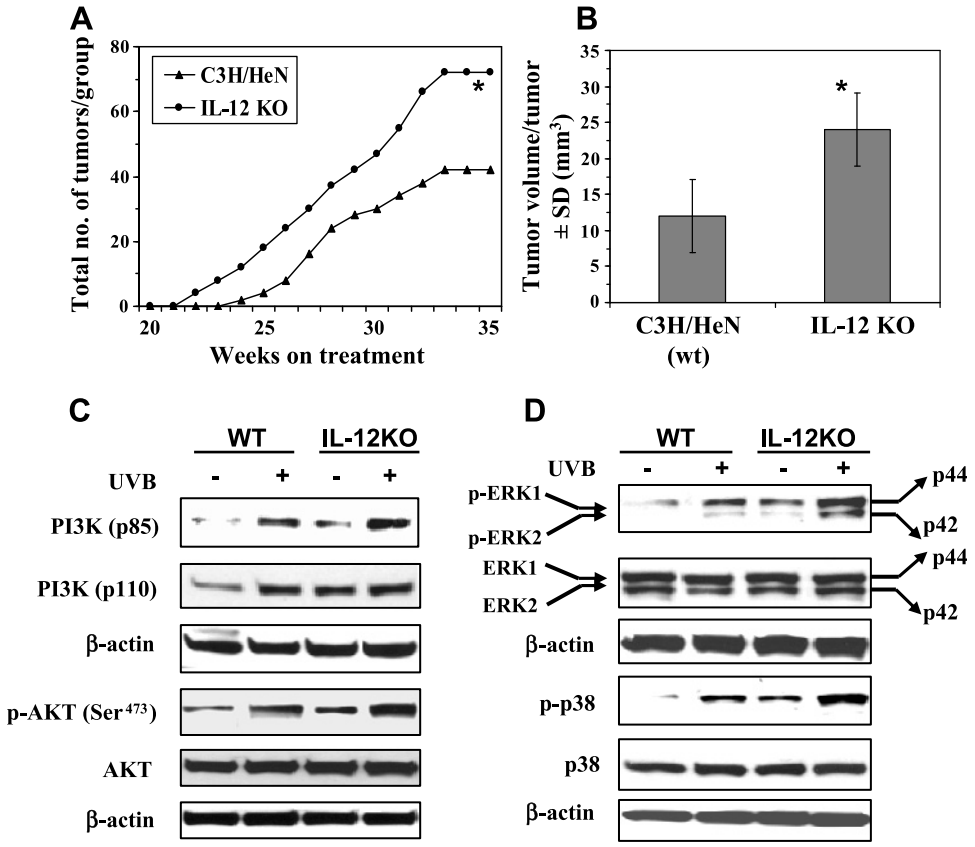

Figure 1. IL-12 deficiency enhances photocarcinogenesis in mice and enhances activation of the cell survival kinases, PI3K, Akt, and MAPK in long-term UV-exposed mouse skin. (A and B) IL-12–deficient mice have a greater number of tumors per group and larger tumor volume/tumor than WT mice, $n = 20$. Significant difference *versus* WT mice, $^*P < .001$. (C) The expression levels of PI3Kp85 (regulatory) and PI3Kp110 (catalytic) and the phosphorylation of Akt (Ser^{473}) are enhanced in UV-exposed skin, and there is greater enhancement in the UVB-exposed IL-12–deficient mouse skin than in the UVB-exposed WT mouse skin. (D) The phosphorylation of ERK1/2 and p38 proteins is enhanced in long-term UV-exposed skin, and this effect is more pronounced in the UVB-exposed IL-12–deficient mouse skin than in the UVB-exposed WT mouse skin. Data were compared with those obtained using skin samples from age-matched non–UVB-exposed control mice. Representative blots are shown from three independent experiments in which almost identical results were observed.

and regulatory (p85) subunits of PI3K in IL-12 KO and wild-type mouse skin were higher in the UVB-exposed skin than in the non–UV-exposed control mouse skin, with the levels of these subunits (p110 and p85) being relatively higher in the UV-exposed skin of IL-12–deficient mice compared with the UV-exposed skin of WT mice (Figure 1*C*). Most of the biologic effects of PI3K are mediated through the activation of the downstream target Akt, a prosurvival factor. The data from Western blot analysis revealed that the phosphorylation of Akt (Ser^{473}) was higher in the UVB-exposed skin of IL-12 KO mice than their WT counterparts (Figure 1*C*), although the levels of total Akt remained unchanged in the skin samples from both WT and IL-12 KO mice.

The activation of MAPK/ERK also plays an important role in the antiapoptotic or cell survival effects [9,22–24]. The MAPKs belong to a family of serine/threonine protein kinases and are believed to act as a system that mediates signal transduction from the cell surface to the nucleus. The results of Western blot analysis indicated that the phosphorylation levels of the ERK1/2 (p44 and p42) and p38 proteins of MAPK family in the UV-exposed skin of IL-12 KO and WT mice were higher than those in the skin samples from the non–UV-exposed control mice and that the phosphorylation levels of ERK1/2 and p38 proteins were higher in the long-term UV-exposed skin of IL-12 KO mice than in the UV-exposed skin of WT mice, as shown in Figure 1*D*. Moreover, the basal levels of phosphorylated ERK1/2 and p38 were higher in the normal skin (non–UV-exposed) of IL-12 KO mice than in the normal skin of WT mice. The total amount of ERK1/2 and p38 proteins remained unchanged in both WT and IL-12 KO mice skin samples.

IL-12 Deficiency Enhances Activation of NF-κB/p65 in UV-Exposed Mouse Skin

Activation of MAPK/ERK and PI3K/Akt results in the activation of NF-κB and its downstream targets that regulate cellular proliferation [8,21]. Western blot analysis indicated a marked activation of NF-κB/p65 and its translocation to the nucleus in the UV-exposed skin of both WT and IL-12 KO mice, with greater activation and translocation of NF-κB in the UV-exposed skin of IL-12 KO mice (Figure 2*A*). As shown in Figure 2*B*, the activity of nuclear NF-κB/p65 was significantly higher ($P < .005$) in the UVB-exposed skin of IL-12 KO mice than in the UVB-exposed skin of their WT counterparts. The induction of IKKα has been shown to be essential for UVB-induced phosphorylation and degradation of IκBα. The levels of activation of IKKα were higher in the UVB-exposed skin of mice than in the non–UVB-exposed control mice. Overall, the activation of IKKα and NF-κB proteins was higher in the UVB-exposed skin of IL-12 KO mice than in the UVB-exposed skin of their WT

counterparts. As assessed by Western blot analysis, the degradation of the IκBα protein and translocation of NF-κB to the nucleus further activate their downstream targets such as iNOS, COX-2, and PCNA, as shown in Figure 2*C*. Analysis of the expression of the proliferation- and inflammation-specific proteins, cyclin D1, PCNA, COX-2, and iNOS using real-time PCR (Figure 2*D*) further indicated significantly higher mRNA levels of cyclin D1 ($P < .01$), PCNA ($P < .01$), COX-2 ($P < .05$), and iNOS ($P < .01$) in the UVB-exposed skin of the IL-12 KO mice than those in the UVB-exposed skin of the WT mice (Figure 2*D*).

NF-κB Activation Is an Important Mediator of UVB-Induced Cellular Proliferation in IL-12 KO Mice

As the activation of NF-κB has been shown to regulate cell proliferation, we were interested in further examining the role of NF-κB in IL-12 KO mice in mediating the effect of UVB-induced cellular proliferation. For this purpose, a short-term experiment was conducted using IL-12 KO mice. These mice were exposed to UVB (90 mJ/cm^2) three times on alternate days with or without the treatment of rIL-12 to determine the effects of restoration of IL-12, or oridonin, which

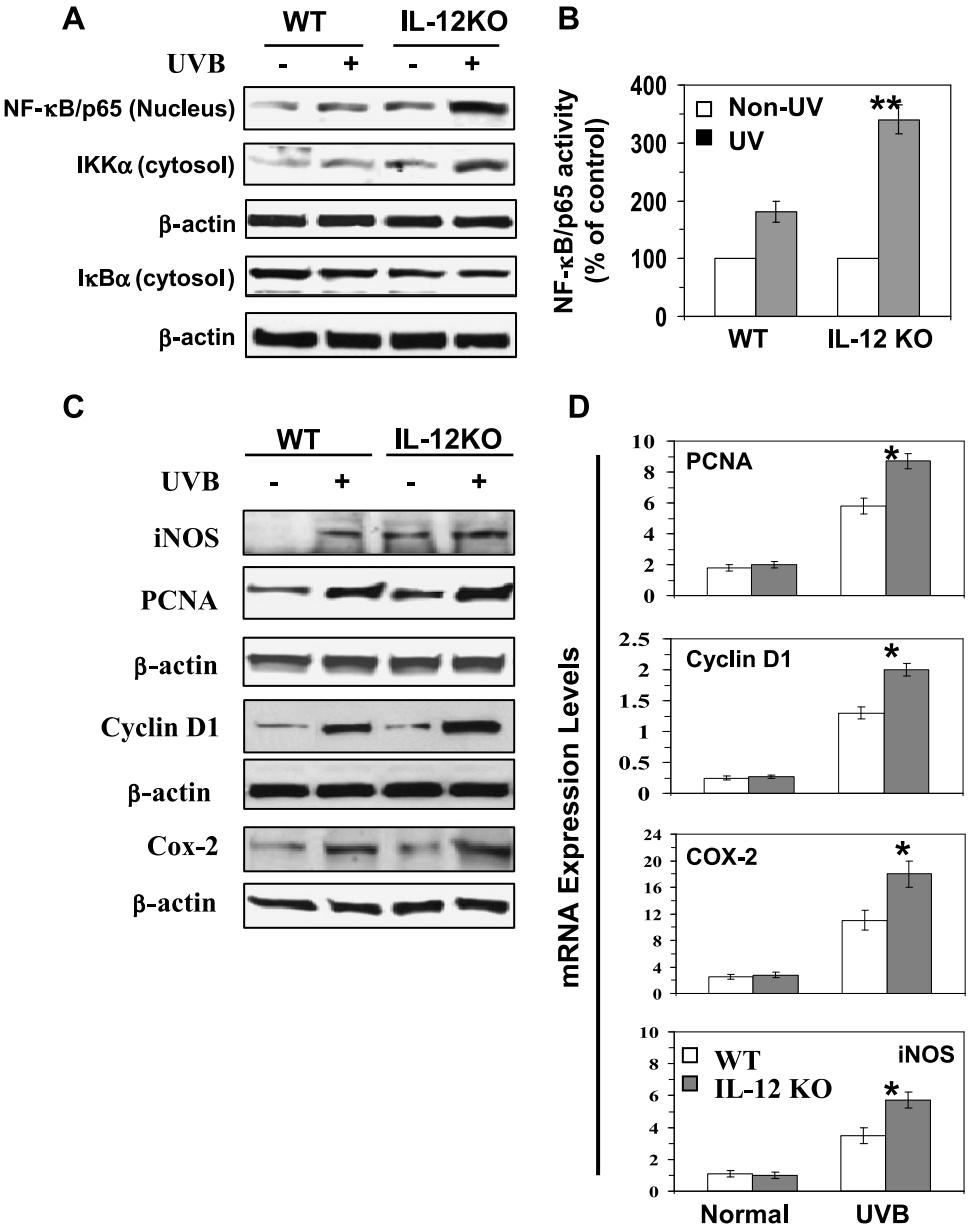

Figure 2. IL-12–deficient mice are more susceptible to UVB-induced activation of NF-κB/p65 and NF-κB–targeted proteins. (A) Long-term UVB exposure of the mouse skin enhances the activation of NF-κB and IKKα, and this effect is greater in the skin of IL-12 KO mice than that of WT mice. (B) The activity of NF-κB in the nuclear fraction of epidermal lysates was measured using NF-κB/p65–specific activity assay kit, $n = 6$. (C) UVB-induced activation of NF-κB–targeted proteins, such as iNOS, cyclin D1, PCNA, and COX-2, is greater in the skin of IL-12–deficient mice than in their wild-type counterparts. Epidermal skin lysates from long-term UV-exposed WT and IL-12 KO mouse skin were used for Western blot analysis. The expression levels of these proteins were also compared with non–UVB-exposed age-matched control mice. A representative blot is shown from three independent experiments with almost identical observations. (D) The total epidermal mRNA expression of PCNA, cyclin D1, COX-2, and iNOS was determined using real-time PCR as described in the Materials and Methods section. The results are presented as the expression of the individual mRNA with normalization to β-actin using the C_t method, $n = 6$. Skin samples from age-matched mice that were not UV irradiated were used as a control. Significant difference *versus* UV-exposed WT mice, $^*P < .01$; $^{**}P < .005$.

downregulates the expression of NF-κB. Mice were killed 24 hours after the last UVB exposure, and skin samples were collected and used for analysis. The results from Western blot analysis indicated that the exposure of IL-12 KO mice to UVB resulted in the activation of IKKα and degradation of IκBα, which leads to the activation of NF-κB and its translocation to the nucleus. Topical treatment of mice with oridonin reduced UVB-induced activation of NF-κB and IKKα, which was followed by enhancement of the levels of IκBα, in IL-12 KO mice (Figure 3*A*). The NF-κB/p65 activity was also significantly reduced ($P < .001$) in the oridonin-treated UVB-exposed IL-12 KO mouse skin (Figure 3*B*). Significant inhibition in the mRNA levels of PCNA and cyclin D1 ($P < .001$) was observed in the oridonin-treated UVB-exposed skin of IL-12 KO mice compared with that in the non–oridonin-treated but UVB-exposed IL-12 KO mice. To further verify our results, the IL-12 KO mice were subcutaneously treated with rIL-12 at the UVB-exposed skin sites using an experimental experiment protocol that was, in all other respects, identical to that used for the analysis of the effects of oridonin treatment. As shown in Figure 3, identical results were obtained with the treatment of IL-12 KO mice with rIL-12 as were obtained on the treatment of IL-12 KO mice with oridonin (Figure 3, *A*–*D*). Thus, the treatment of IL-12 KO mice with either subcutaneous injection of rIL-12 or topical application of oridonin resulted in the inhibition of NF-κB expression in UVB-exposed IL-12 KO mice, and this was followed by a reduction in the expression of markers of cellular proliferation (PCNA and cyclin D1). Importantly, the inhibition of UVB-induced expression of NF-κB, PCNA, and cyclin D1 after the subcutaneous administration of rIL-12 to IL-12 KO mice also suggested a photoprotective role of IL-12 on UVB-induced adverse effects.

IL-12 Deficiency in Mice Enhances the Levels of PI3K/Akt, MAPKs, and NF-κB Expression in UVB-Induced Skin Tumors

We further analyzed the expression levels of cell survival kinases and NF-κB in the UVB-induced skin tumors of WT and IL-12 KO mice. For this purpose, we used the papillomas for making the tumor lysates. Similar to the patterns of expression that we had observed in the long-term UVB-exposed mouse skin, we found that the levels of PI3K, both regulatory (p85) and catalytic (p110) protein subunits, and the downstream activation of Akt (p-Akt at Ser^{473}) were higher in the UVB-induced tumors of IL-12 KO mice than in the UVB-induced tumors of their WT counterparts (Figure 4*A*). The phosphorylation of ERK1/2 (p44 and p42) and p38 proteins of the MAPK family was also higher in the UVB-induced tumors of IL-12 KO mice

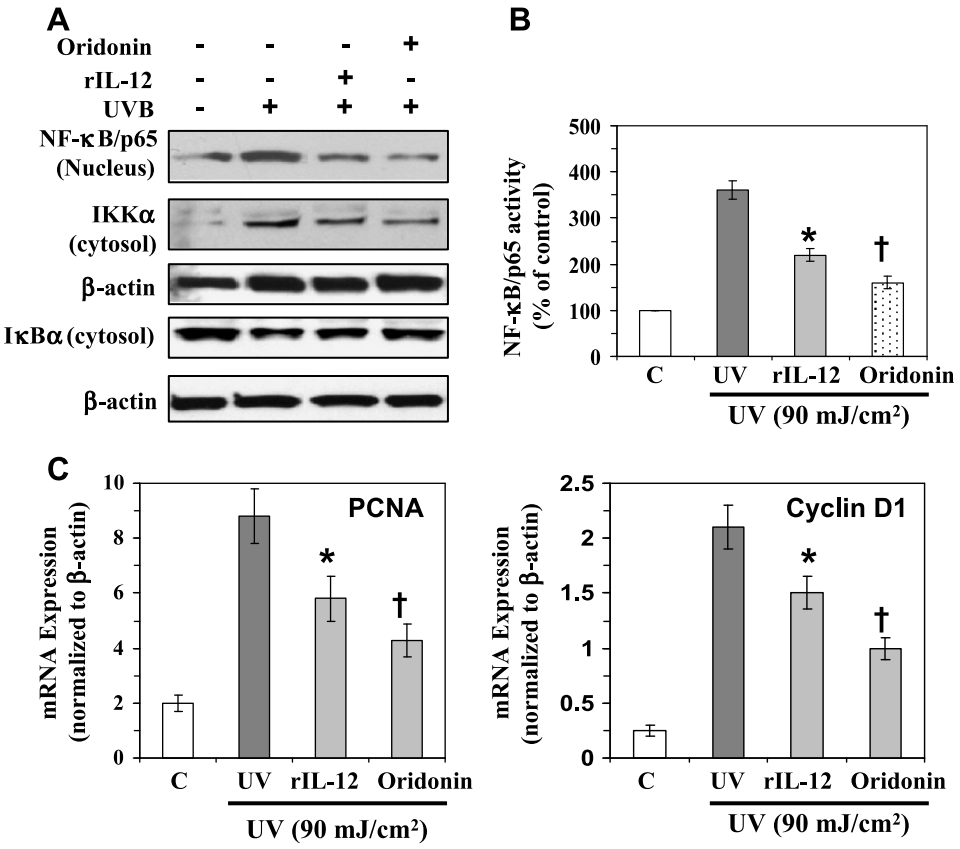

Figure 3. Inhibition of UVB-induced activation of NF-κB in IL-12 KO mice reduces the proliferation potential of epidermal cells. Oridonin (20 μmol), a NF-κB inhibitor, was topically applied on the shaved back of IL-12 KO mice 30 minutes before each UVB exposure. Another group of IL-12 KO mice was injected subcutaneously with rIL-12 (1000 ng per mouse) at the site of UV irradiation 3 hours before each UVB exposure. (A) Epidermal skin lysates were used for Western blot analysis. The NF-κB/p65 expression was measured in the epidermal nuclear extract using Western blot analysis as detailed in the Materials and Methods section. (B) The activity of NF-κB/p65 in the nuclear fraction of epidermal skin was measured using NF-κB/p65–specific activity assay kit. Age-matched and non–UV-exposed IL-12 KO mice served as controls, $n = 6$. (C) Analysis of mRNA levels of PCNA and cyclin D1 using real-time PCR as described in the Materials and Methods section. Significant inhibition *versus* UVB exposure alone, $^{*}P < .05$; $^{\dagger}P < .001$.

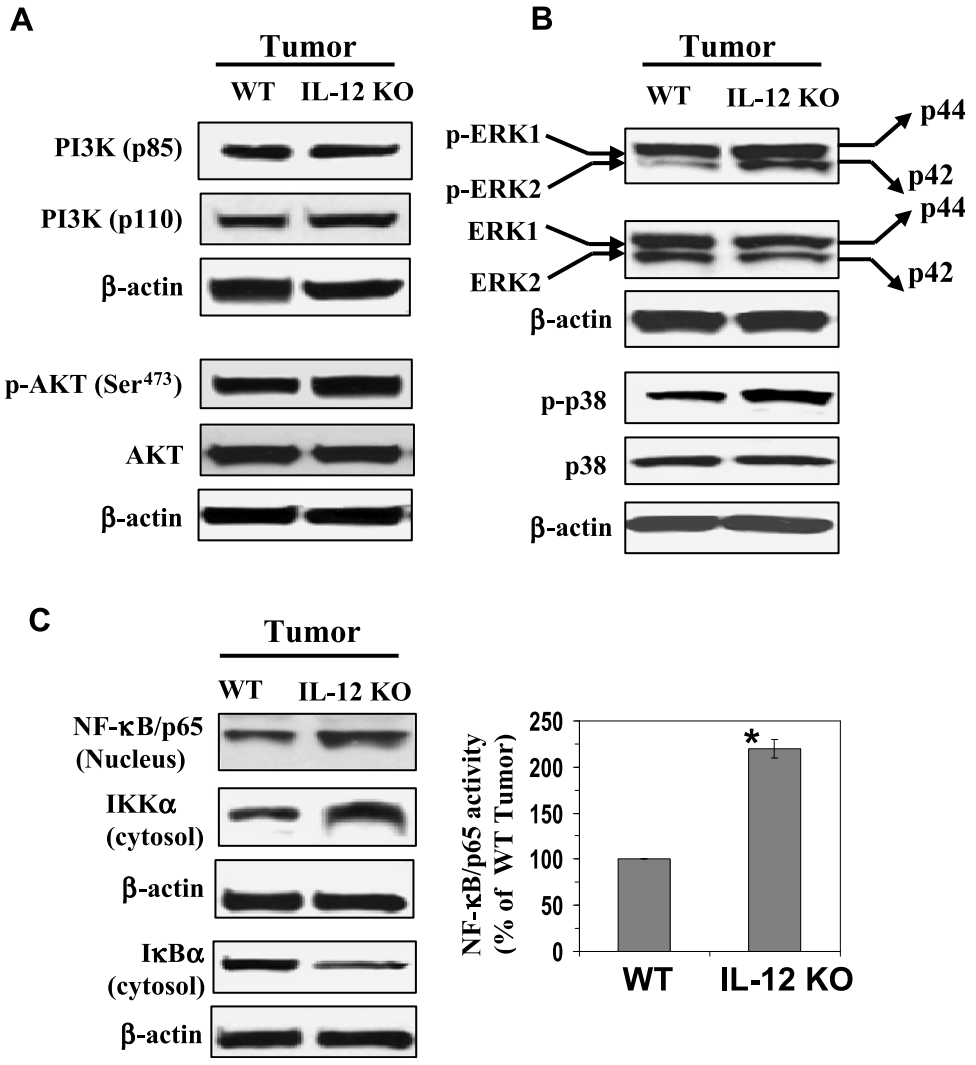

Figure 4. IL-12 deficiency enhances the activation of cell survival kinases PI3K, Akt, and MAPK and the activation of NF-κB in UV-induced skin tumors. Tumor samples were obtained from the photocarcinogenesis experiment (Figure 1) as detailed in the Materials and Methods section. Tumor lysates were subjected to Western blot analysis for the measurement of various cell survival kinase proteins. (A) The expression levels of PI3Kp85 (regulatory) and PI3Kp110 (catalytic) and the phosphorylation of Akt (Ser^{473}) are higher in the UVB-induced skin tumors of IL-12–deficient mice than in the UVB-induced skin tumors of WT mice. (B) The phosphorylation of ERK1/2 (p44 and p42) and p38 proteins in UV-induced skin tumors is greater in the UVB-induced skin tumors of IL-12–deficient mice than in the UVB-induced skin tumors of WT mice. (C) The activation of NF-κB and IKKα is greater in the UVB-induced skin tumors than in the UVB-induced skin tumors of WT mice. In each case, a representative blot is shown. A total of 10 mice were used for Western blot analysis. The activity of NF-κB/p65 in nuclear fractions of tumors was measured by NF-κB/p65–specific activity assay kit, $n = 6$. Significant difference *versus* wild types, $^*P < .01$.

than in the UVB-induced tumors of WT mice (Figure 4*B*). The expression levels of total Akt, ERK1/2, and p38 were similar in the UVB-induced tumors of the WT and IL-12 KO mice (Figure 4, *A* and *B*), and equal protein loading was confirmed by reprobing the membranes with β-actin.

Examination of the activation profile of NF-κB and the proteins of the NF-κB family by Western blot analysis indicated that the activation of NF-κB/p65 (nucleus) and IKKα (cytosol) was greater in the UVB-induced tumors of the IL-12 KO mice than in the UVB-induced tumors of WT mice. In contrast, the levels of IκBα were lower in the UVB-induced tumors of the IL-12 KO mice that in the UVB-induced tumors of WT mice (Figure 4*C*). The activity of NF-κB/p65 in the nuclear fraction was also measured using NF-κB/p65–specific activity assay kit and was significantly greater ($P < .001$) in the UVB-induced skin tumors of IL-12 KO mice than in the UVB-induced skin tumors of WT mice (Figure 4*C*). Taken together, these results suggest that lack of endogenous IL-12 results in enhanced activation of cell survival signals in UVB-induced skin tumors and that this may be associated with the more rapid growth and larger size of tumors in the IL-12 KO mice than in their WT counterparts.

IL-12 Deficiency in Mice Increases Tumor Cell Proliferation and Inhibits Apoptosis in UVB-Induced Skin Tumors

Our results suggested that enhanced activation of cell survival signals in UVB-induced skin tumors associated with the lack of endogenous IL-12 may, in turn, be associated with the more rapid growth and larger size of tumors in the IL-12 KO mice than in their WT counterparts. Further examination of this issue was of some importance because IL-12 deficiency enhances photocarcinogenesis in mice [2,3]. Analysis of the apoptotic index of tumors using the TUNEL assay clearly

indicated that the percentage of apoptotic cells (TUNEL$^+$ cells) were significantly lower (31%, $P < .05$) in the UVB-induced tumors of IL-12 KO mice compared with the UVB-induced tumors of WT mice (Figure 5, *A* and *B*). To verify this observation, we also checked the numbers of activated caspase 3$^+$ cells in tumors (a biomarker of apoptotic cell death) using immunostaining. As shown in Figure 5 (*A* and *B*, *middle panels*), the immunostaining and subsequent analysis in the percentage of activated caspase 3$^+$ cells in the tumors indicated that the percentage of caspase 3$^+$ cells in the UVB-induced tumors of IL-12 KO mice were significantly lower (63%, $P < .01$) than the numbers in the UVB-induced tumors of WT mice. Together, these results indicated that IL-12 deficiency in mice inhibits the apoptotic cell death in UVB-induced tumors and, by extension, that the endogenous IL-12 promotes apoptotic cell death in UV-induced skin tumors. The results of activated caspase 3 data were further verified by Western blot analysis using tumor lysates, which also suggested that the levels of activated caspase 9 and caspase 3 proteins were lower in the UVB-induced tumors of IL-12 KO mice than in their WT counterparts (Figure 5*C*). In contrast, the cellular proliferation in the percentage of PCNA$^+$ cells in tumors of IL-12 KO mice was significantly higher (40%, $P < .05$) than in the tumors of WT mice, as analyzed by immunostaining (Figure 5, *A* and *B*, *bottom panels*). Figure 5*C* also shows the expression levels of some of the surrogate markers of apoptosis in tumors of WT and IL-12 KO mice. The phosphorylation of Bad (Ser^{136}) was higher in

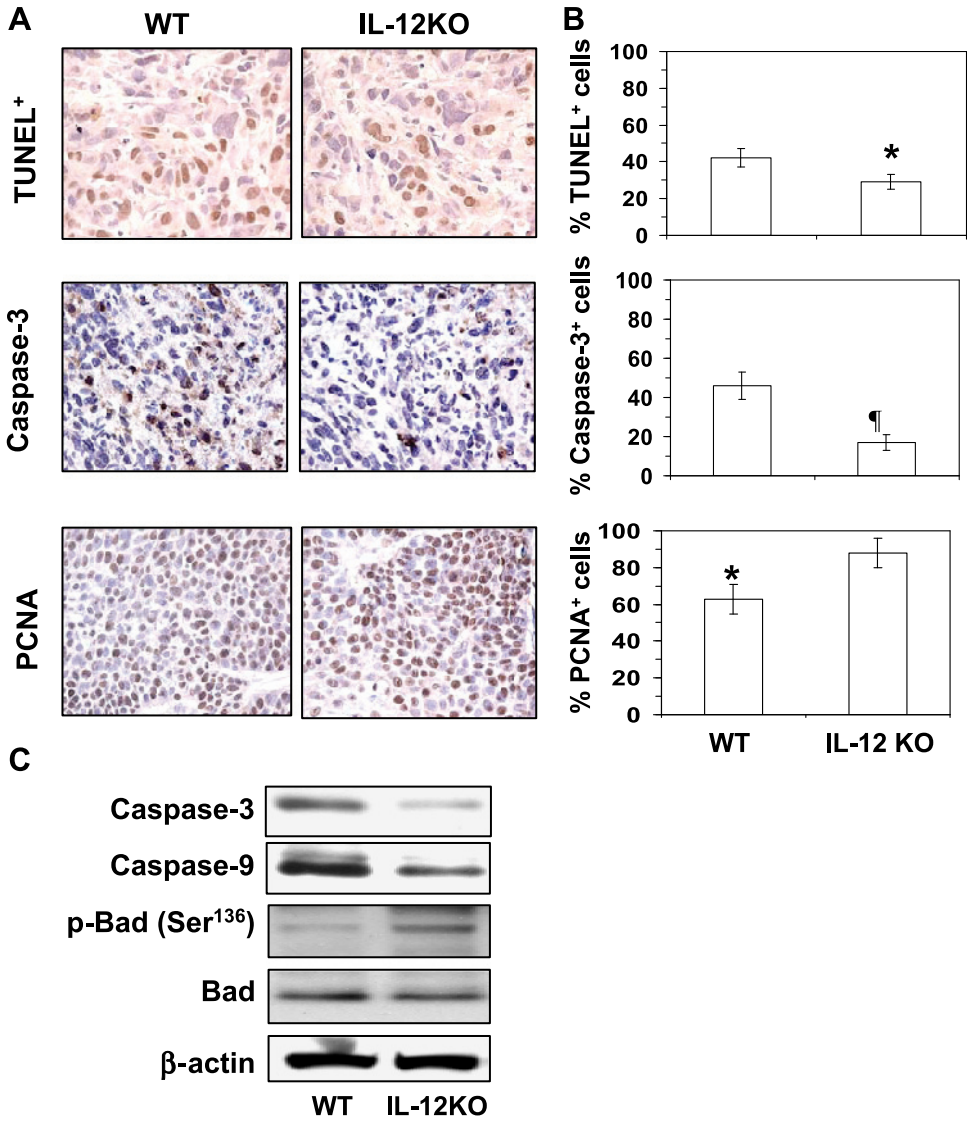

Figure 5. IL-12 deficiency inhibits apoptosis in UV-induced skin tumors. At the termination of the photocarcinogenesis experiment (Figure 1), mice were killed, and skin tumors were collected for the analysis of apoptosis indices. (A) Detection and analysis of apoptotic cells in tumors as identified by the TUNEL assay and immunostaining for activated caspase 3–positive cells. The proliferation potential of cells in skin tumors was estimated by immunostaining for PCNA. Immunostaining-positive cells are shown as dark brown. (B) The presence of apoptotic cells, caspase 3–positive cells, and PCNA-positive cells in tumors of IL-12 KO and WT mice was counted and summarized in percentage of total cells. Data represent the mean ± SEM ($n = 6$). Significant difference *versus* WT mouse, *$P < .05$; ¶$P < .01$. (C) Tumor lysates were used to analyze the levels of activated caspase 9, caspase 3, and p-Bad (Ser^{136}) in the skin tumors of IL-12 KO and in their WT counterparts using Western blot analysis. The representative blots are shown from three independent experiments, and in each experiment, the tumor samples were pooled from at least three mice for preparation of lysates ($n = 10$), and equivalent protein loading was checked by probing stripped blots for β-actin as shown.

the UVB-induced tumors of IL-12 KO mice than in the UVB-induced tumors of WT mice (Figure 5*C*). The relatively lower expression of the proapoptotic protein Bad and increased level of p-Bad (Ser^{136}) might be due to the activation of Akt at Ser^{473} in the UVB-induced tumors of the IL-12 KO compared with the UVB-induced tumors of WT mice. These data suggest that this may be the reason that IL-12 KO mice develop more tumors in UV-exposed skin than their wild-type counterparts [2,3] and suggest that the endogenous IL-12 in the IL-12–proficient mice (WT) contributes to their development of fewer tumors on exposure to a UVB carcinogenesis protocol.

Discussion

Previously, we and others showed that a deficiency of IL-12 enhances the risk of photocarcinogenesis in mice [2,3] suggesting that IL-12 possesses antiphotocarcinogenic activities. Cell survival signals, including the PI3K/Akt, MAPK, and NF-κB signaling pathways, have been associated with cellular proliferation and carcinogenesis [10,19,20]. Therefore, in this study, we investigated the effects of IL-12 deficiency on PI3K/Akt, MAPK, and NF-κB signaling in UVB-exposed skin and skin tumors with the goal of gaining insights into the mechanisms that link the lack of endogenous IL-12 with the rapid growth of skin tumors and the multiplicity of these tumors in UVB-exposed IL-12 KO mice and the mechanisms by which endogenous IL-12 may afford some protection against UVB-induced photocarcinogenesis in mice.

It is well established that activation of PI3K can play an important role in carcinogenesis [20,25,26]. The biologic effects of PI3K are mediated through the activation or phosphorylation of the downstream target, Akt. Akt, also known as protein kinase B, is a serine/threonine kinase, which has been identified as an important component of pro-survival signaling pathways [27]. Our study demonstrates that long-term exposure of mice to UVB radiation enhances the activation of PI3K and Akt in both IL-12–deficient and WT mice. However, the UVB-induced activation of PI3K and Akt was higher in the IL-12–deficient mice than in the WT mice. The PI3K/Akt signaling pathway regulates the activity of the transcriptional factor, NF-κB, which in turn is known to regulate several well-known markers of tumor promotion and tumor cell proliferation, for example, COX-2, iNOS, PCNA, and cyclin D1 [28,29]. Our study clearly demonstrates that exposure of mice to UVB radiation induces the expression of both regulatory (p85) and catalytic (p110) subunits of PI3K and activates Akt by phosphorylation at Ser^{473} in both IL-12/23–deficient and WT mice, with these effects being more pronounced in the IL-12–deficient mice than in their WT counterparts. The greater activation of PI3K/Akt pathway in the skin of the IL-12 KO mice has the potential to promote cell survival by activating the NF-κB signaling pathway [30]. Thus, the greater susceptibility of the IL-12 KO mice to photocarcinogenesis may be mediated, at least in part, through greater activation of the PI3K/Akt pathway.

The activation of NF-κB, which has been implicated in inflammation, cell proliferation, and oncogenic processes [31,32], depends on the phosphorylation and subsequent degradation of IκB proteins. Our study showed that long-term exposure to UVB irradiation enhances the activation of NF-κB/p65 in the skin of IL-12–deficient and WT mouse skin and simultaneously enhances the expression of IKKα while inhibiting the degradation of IκBα. These effects are more pronounced in the skin of IL-12 KO mice. The activation of NF-κB has been shown to upregulate the expression of proinflammatory cytokines and inflammatory and oxidative gene products, such as COX-2 and iNOS [23,33], as well as key regulators of cell proliferation, most notably its effects on cell cycle progression, including its effects on cyclin D1, a cyclin that is expressed early in the cell cycle and is important for DNA synthesis [24]. Most of these genes have been shown to be upregulated in human cancers, suggesting that up-regulation of NF-κB and subsequent up-regulation of NF-κB–targeted genes may promote the development of cancers. In this study, we observed that UVB exposure of IL-12–deficient and WT mouse skin markedly upregulated the expression of NF-κB–responsive proteins, such as COX-2, iNOS, cyclin D1, and PCNA, and that this effect was more pronounced in the UVB-exposed skin of the IL-12 KO mice than the UVB-exposed skin of WT mice. The up-regulation of these NF-κB–targeted proteins in the UVB-exposed skin of IL-12 KO mice may explain the susceptibility of the IL-12–deficient mice to photocarcinogenesis. As it is well known that the NF-κB pathway has a role in cell survival and proliferation, our findings suggest that the enhanced photocarcinogenesis in IL-12–deficient mice may be due to the enhanced activation of NF-κB.

We observed that long-term exposure to UVB radiation stimulates the phosphorylation of MAPK proteins in IL-12–deficient mice to a greater extent than long-term UVB exposure of WT mouse skin. The higher levels of phosphorylation of MAPK proteins play a major role in cell growth, differentiation, and proliferation and may lead to clonal expansion of tumor cells into tumors [9]. The MAPK signaling pathway is an important upstream regulator of the activity of transcription factors implicated in carcinogenesis [34]. Our Western blot data demonstrate that the expression levels of UVB-induced phosphorylated proteins of MAPK family, such as ERK1/2 and p38, in IL-12 KO mouse skin were higher than those in the skin of WT mice. The phosphorylation of ERK1/2 has been shown to play a critical role in transmitting signals from extracellular to intracellular molecules. Phosphorylation of ERK1/2 and p38 also influences the activation of inflammation and progression of various types of tumors. Therefore, the increase in the expression of phosphorylation of MAPK proteins after UVB irradiation of mice may, in turn, enhance the downstream events, such as activation of NF-κB that can contribute to the development of skin cancers. We suggest that comparatively higher phosphorylation of MAPK proteins in the UVB-exposed skin of IL-12 KO mice than WT mice might be responsible for their stimulatory effects on the activation of transcription factor NF-κB. Because activation of NF-κB plays a critical role in tumor promotion, we further verified its effect by treating the IL-12 KO mice subcutaneously with rIL-12 or with topical application of oridonin, an inhibitor of NF-κB. We found that subcutaneous treatment of IL-12 KO mice with rIL-12 resulted in the inhibition of UVB-induced activation of NF-κB and in the subsequent inhibition of the expression levels of PCNA and cyclin D1. These data add new information that restoration of IL-12 in IL-12 KO mice reverses the photodamaging effects of UV radiation. Similar effects were also obtained when these mice were treated with oridonin. This set of data suggests that if the IL-12 deficiency is corrected or if the activation of NF-κB is inhibited, then the process of cellular proliferation can be reduced.

We further checked the effects of IL-12 deficiency on the kinase pathways in UVB-induced skin tumors. It was observed that the pattern of enhancement of cell survival signals, including the expression levels of PI3K/Akt, MAPK, and NF-κB, in the UVB-induced tumors was identical to those found in the long-term UVB-exposed skin of the IL-12 KO and WT mice. Analysis of the UVB-induced tumors further confirmed that the numbers of TUNEL-positive and activated

caspase 3–positive cells were significantly lower in the UVB-induced tumors of IL-12 KO mice than the UVB-induced tumors of WT mice. In addition, the proliferation potential of tumor cells in the percentage of PCNA-positive cells was higher in the UVB-induced tumors of IL-12 KO mice than in the UVB-induced tumors of WT mice.

Together, the present findings suggest that endogenous IL-12 deficiency promotes the UVB-induced cell survival signals in mouse skin and that this may be a contributing factor in the early, rapid, and enhanced development of skin tumors induced by UVB exposure of IL-12 KO mouse skin. In other words, stimulation of endogenous IL-12 may downregulate the cell survival signals in the skin and tumors and thus may inhibit or retard UV carcinogenesis. Further, it is suggested that endogenous enhancement of IL-12 may be considered as an effective strategy for the prevention of UV irradiation–associated skin diseases including skin cancers.

References

[1] Trinchieri G (1994). Interleukin-12 a cytokine produced by antigen-presenting cells with immunoregulatory functions in the generation of T-helper cells type 1 and cytotoxic lymphocytes. *Blood* **84**, 4008–4027.

[2] Meeran SM, Mantena SK, Meleth S, Elmets CA, and Katiyar SK (2006). Interleukin-12–deficient mice are at greater risk of ultraviolet radiation–induced skin tumors and malignant transformation of papillomas to carcinomas. *Mol Cancer Ther* **5**, 825–832.

[3] Maeda A, Schneider SW, Kojima M, Beissert S, Schwarz T, and Schwarz A (2006). Enhanced photocarcinogenesis in interleukin-12–deficient mice. *Cancer Res* **66**, 2962–2969.

[4] Meeran SM, Katiyar S, Elmets CA, and Katiyar SK (2007). Interleukin-12 deficiency is permissive for angiogenesis in UV radiation–induced skin tumors. *Cancer Res* **67**, 3785–3793.

[5] Katiyar SK (2007). Interleukin-12 and photocarcinogenesis. *Toxicol Appl Pharmacol* **224**, 220–227.

[6] Schwarz A, Ständer S, Berneburg M, Böhm M, Kulms D, van Steeg H, Grosse-Heitmeyer K, Krutmann J, and Schwarz T (2002). Interleukin-12 suppresses ultraviolet radiation–induced apoptosis by inducing DNA repair. *Nat Cell Biol* **4**, 26–31.

[7] Tyrrell RM (1996). Activation of mammalian gene expression by the UV component of sunlight—from models to reality. *Bioessays* **18**, 139–148.

[8] Sharma SD, Meeran SM, and Katiyar SK (2007). Dietary grape seed proanthocyanidins inhibit UVB-induced oxidative stress and activation of mitogen-activated protein kinases and nuclear factor-κB signaling in *in vivo* SKH-1 hairless mice. *Mol Cancer Ther* **6**, 995–1005.

[9] Bode AM and Dong Z (2003). Mitogen-activated protein kinase activation in UV-induced signal transduction. *Sci STKE* **167**, 1–15.

[10] Nomura M, Kaji A, Ma WY, Zhong S, Liu G, Bowden GT, Miyamoto KI, and Dong Z (2001). Mitogen- and stress-activated protein kinase 1 mediates activation of Akt by ultraviolet B irradiation. *J Biol Chem* **276**, 25558–25567.

[11] Datta SR, Brunet A, and Greenberg ME (1999). Cellular survival: a play in three Akts. *Genes Dev* **13**, 2905–2927.

[12] Bargou RC, Emmerich F, Krappmann D, Bommert K, Mapara MY, Arnold W, Royer HD, Grinstein E, Greiner A, Scheidereit C, et al. (1997). Constitutive nuclear factor-κB–RelA activation is required for proliferation and survival of Hodgkin's disease tumor cells. *J Clin Invest* **100**, 2961–2969.

[13] Duffey DC, Chen Z, Dong G, Ondrey FG, Wolf JS, Brown K, Siebenlist U, and Van Waes C (1999). Expression of a dominant-negative mutant inhibitor-κBα of nuclear factor-κB in human head and neck squamous cell carcinoma inhibits survival, proinflammatory cytokine expression, and tumor growth *in vivo*. *Cancer Res* **59**, 3468–3474.

[14] Pöppelmann B, Klimmek K, Strozyk E, Voss R, Schwarz T, and Kulms D (2005). NFκB-dependent down-regulation of tumor necrosis factor receptor–associated proteins contributes to interleukin-1–mediated enhancement of ultraviolet B–induced apoptosis. *J Biol Chem* **280**, 15635–15643.

[15] Mittal A, Elmets CA, and Katiyar SK (2003). Dietary feeding of proanthocyanidins from grape seeds prevents photocarcinogenesis in SKH-1 hairless mice: relationship to decreased fat and lipid peroxidation. *Carcinogenesis* **24**, 1379–1388.

[16] Leung CH, Grill SP, Lam W, Han QB, Sun HD, and Cheng YC (2005). Novel mechanism of inhibition of nuclear factor-κ B DNA-binding activity by diterpenoids isolated from *Isodon rubescens*. *Mol Pharmacol* **68**, 286–297.

[17] Meeran SM, Punathil T, and Katiyar SK (2008). Interleukin-12–deficiency exacerbates inflammatory responses in UV-irradiated skin and skin tumors. *J Invest Dermatol* **128**, 2716–2727.

[18] Brunda MJ, Luistro L, Warrier RR, Wright RB, Hubbard BR, Murphy M, Wolf SF, and Gately MK (1993). Antitumor and antimetastatic activity of interleukin-12 against murine tumors. *J Exp Med* **178**, 1223–1230.

[19] Saleem M, Afaq F, Adhami VM, and Mukhtar H (2004). Lupeol modulates NF-κB and PI3K/Akt pathways and inhibits skin cancer in CD-1 mice. *Oncogene* **23**, 5203–5214.

[20] Luo J, Manning BD, and Cantley LC (2003). Targeting the PI3K-Akt pathway in human cancer: rationale and promise. *Cancer Cell* **4**, 257–262.

[21] Meeran SM and Katiyar SK (2008). Proanthocyanidins inhibit mitogenic and survival-signaling *in vitro* and tumor growth *in vivo*. *Front Biosci* **13**, 887–897.

[22] Rengifo-Cam W, Umar S, Sarkar S, and Singh P (2007). Antiapoptotic effects of progastrin on pancreatic cancer cells are mediated by sustained activation of nuclear factor-κB. *Cancer Res* **67**, 7266–7274.

[23] Baldwin AS (2001). Control of oncogenesis and cancer therapy resistance by the transcription factor NF-κB. *J Clin Invest* **107**, 241–246.

[24] Guttridge DC, Albanese C, Reuther JY, Pestell RG, and Baldwin AS Jr (1999). NF-κB controls cell growth and differentiation through transcriptional regulation of cyclin D1. *Mol Cell Biol* **19**, 5785–5799.

[25] Mills GB, Kohn E, Lu Y, Eder A, Fang X, Wang H, Bast RC, Gray J, Jaffe R, and Hortobagyi G (2003). Linking molecular diagnostics to molecular therapeutics: targeting the PI3K pathway in breast cancer. *Semin Oncol* **30**, 93–104.

[26] Osaki M, Kase S, Adachi K, Takeda A, Hashimoto K, and Ito H (2004). Inhibition of the PI3K-Akt signaling pathway enhances the sensitivity of Fas-mediated apoptosis in human gastric carcinoma cell line, MKN-45. *J Cancer Res Clin Oncol* **130**, 8–14.

[27] Downward J (1998). Mechanisms and consequences of activation of protein kinase B/Akt. *Curr Opin Cell Biol* **10**, 262–267.

[28] Callejas NA, Casado M, Bosca L, and Martin-Sanz P (1999). Requirement of nuclear factor κB for the constitutive expression of nitric oxide synthase-2 and cyclooxygenase-2 in rat trophoblasts. *J Cell Sci* **18**, 3147–3155.

[29] Carpenter CL and Cantley LC (1996). Phosphoinositide kinases. *Curr Opin Cell Biol* **8**, 153–158.

[30] Romashkova JA and Makarov SS (1999). NF-κB is a target of AKT in antiapoptotic PDGF signaling. *Nature* **401**, 86–90.

[31] Thanos D and Maniatis T (1995). NF-κ B: a lesson in family values. *Cell* **80**, 529–532.

[32] Baeuerle PA and Baltimore D (1996). NF-κ B: ten years after. *Cell* **87**, 13–20.

[33] Rayet B and Gelinas C (1999). Aberrant *rel/nfkb* genes and activity in human cancer. *Oncogene* **18**, 6938–6947.

[34] McCarty MF (1998). Polyphenol-mediated inhibition of AP-1 transactivating activity may slow cancer growth by impeding angiogenesis and tumor invasiveness. *Med Hypotheses* **50**, 511–514.